THERMODYNAMIC MODELING OF ADSORPTION AT THE LIQUID-SOLID INTERFACE

Rajasi Shukre[1], Shikha Bhaiya[1], Usman Hamid[1], Hla Tun[1], and Chau-Chyun Chen[1]

[1]*Department of Chemical Engineering, Texas Tech University, Lubbock, Texas 79409, United States*

ABSTRACT

Adsorption based separation techniques are significantly energy efficient in comparison to the conventional thermal separation techniques such as distillation. Despite the extensive research and development activities undertaken for mixed gas adsorption, the use of adsorption techniques for the separation of multicomponent liquid mixtures is still limited. This is due to the lack of accurate adsorption thermodynamic models, which form the scientific foundation of process simulation of such systems, making the translation to the industrial scale challenging. In this work, we have rigorously computed the surface excess of adsorption for six binary liquid mixtures on silica gel at 303 K using the frameworks of the adsorbed solution theory and the generalized Langmuir isotherm model. The six binary liquid mixtures studied in this work were formed by the pair-wise combinations of four components : benzene, 1,2-dichloroethane, cyclohexane and n-heptane. We have based our calculations by considering simultaneous equilibria of three phases : saturated binary vapor phase, binary liquid phase and the adsorbed phase. The composition of the corresponding saturated vapor phase was determined by correlating the experimental vapor-liquid equilibria data using the Non-Random Two-Liquid activity coefficient model. The activity coefficients of the adsorbed phase were calculated using the adsorption Non-Random Two-Liquid activity coefficient model. Devoid of simplifying assumptions, our methodology for computing the surface excess of binary liquid adsorption should be applicable for the adsorption from a wide variety of liquid mixtures.

1. INTRODUCTION

The selective separation of bulk liquid mixtures has been traditionally performed through distillation [1]. There are twofold reasons for this convention. The first reason is that there is a vast amount of literature data available for the vapor-liquid equilibria for a variety of liquid mixtures. Secondly, the thermodynamics of vapor-liquid equilibria is a well-established field, with a number of activity coefficient models describing the behavior of non-ideal mixtures exhibiting large deviations from Raoult's law [2]. Thus, the process simulation, design and optimization of a distillation column has been a long-standing, ubiquitous process. However, the major disadvantage of conventional distillation operation is the cost associated with the reboiler and condenser duty, making this legacy separation process energy-intensive [3].

Adsorption processes have been shown to be highly energy efficient as compared to distillation processes, with higher separation efficiencies even for azeotropic mixtures [4]. Although the process simulations and implementation of adsorption processes have been widely studied for the separation of gas mixtures, such wide-scale research and practice is still missing for the separation of bulk liquid mixtures [5, 6]. In the latter case, there is also a scarcity of experimental surface excess data [6]. Therefore, there has not been much work reported on the thermodynamic modeling front for bulk liquid adsorption processes, making the design and implementation even more challenging.

Some of the early studies on the thermodynamic modeling of adsorption from bulk liquid solutions come from the contributions made by Everett and co-workers, who recognized the correlation between adsorption at the solid-vapor and the solid-solution interface [7]. However, the derived correlations for surface excess were based on several assumptions related to the monolayer structure of the adsorbed phase, nature of the bulk liquid phase and orientation of the adsorbed molecules on the adsorbent surface [7–16] , which in turn severely limited the applicability of such models.

The systematic investigation of the thermodynamics of liquid adsorption has been reported by Myers, Sircar and co-workers who developed fundamental expressions for the thermodynamic excess functions associated with liquid adsorption [17]. They measured the surface excess of several liquid mixtures on silica gel, activated carbon, titanium dioxide as well as graphon and developed a thermodynamic consistency test for the experimental data of surface excess [18,19].

Moreover, they developed a rigorous framework to correlate the adsorption of liquid mixtures to the adsorption of the corresponding vapor mixtures, in the limit of saturation [20]. However, the derivation of the subsequent surface excess expression was based on the assumption of an ideal adsorbed phase [21]. The calculation of the surface excess required sequential solving of multiple equations [22]. Adsorbent heterogeneity was accounted for by the monolayer pore filling model, coupled with distribution function for site selectivities resulting in a complex expression for the surface excess. [23].

Thus, it can be seen that prior thermodynamic models in the literature are based on simplifying assumptions and there is a crucial need to develop models that consider the activity coefficients of the adsorbed phase at the liquid-solid interface. Therefore, in this work, we have developed a rigorous thermodynamic framework to estimate the adsorption of binary liquid mixtures using the ideal adsorbed solution theory (IAST) and the real adsorbed solution theory (RAST) [8, 24]. For the latter, we have implemented the adsorption Non-Random Two-Liquid (aNRTL) model for evaluating the adsorbed phase activity coefficients [25]. We have also performed the surface excess computations using the recently developed generalized Langmuir isotherm model (gL) [26]. The framework of the gL isotherm model does not require the calculation of the spreading pressure of the adsorption system, making the implementation computationally inexpensive.

We have based our calculations on the equivalence of adsorption from binary liquid mixtures and adsorption from the corresponding saturated binary vapor mixtures, as developed by Myers and Sircar [20]. The saturation pressure and the composition of the corresponding saturated vapor phase was evaluated using the Non-Random Two-Liquid (NRTL) activity coefficient model [27]. We have tested our thermodynamic framework for the adsorption of six binary liquid mixtures on silica gel at 303 K : *i*) benzene−1,2-dichloroethane, *ii*) benzene−cyclohexane, *iii*) cyclohexane−1,2-dichloroehtane, *iv*) benzene−n-heptane,, *v*) cyclohexane−n-heptane, *vi*) 1,2-dichloroethane−n-heptane [6,18]. These systems were selected because the pure component vapor isotherm data for each of the four components on silica gel at 303 K was available [6,18].

We have successfully correlated the surface excess for all six binary systems, resulting in a good agreement with the experimental surface excess data using the IAST and RAST frameworks. The gL model represented the trend of the data qualitatively for all the systems.

The thermodynamic framework for correlating the adsorption from binary liquid mixtures to the adsorption from the corresponding saturated vapor phase along with discussion of the results of the IAST and RAST frameworks and the gL model are given in the subsequent sections.

2. THERMODYNAMIC FRAMEWORK

2.1 General Methodology

The thermodynamic system for the adsorption of binary liquid mixture consists of three phases, all at equilibrium with one another at a constant temperature T, as shown in Figure 1 [18]. The bulk liquid phase consists of liquid components 1 and 2. Upon contacting the binary liquid mixture with a solid adsorbent, adsorption of the two components occurs to form the adsorbed phase. After establishment of equilibrium between the two phases, the mole fractions of components 1 and 2 in the bulk liquid phase are denoted as x_1 and x_2, respectively, whereas the mole fractions of the two components in the adsorbed phase are denoted as x'_1 and x'_2, respectively. Moreover, the bulk liquid phase is also in equilibrium with its saturated vapor phase at the given temperature, with vapor phase mole fractions denoted as y_1 and y_2 for the components 1 and 2, respectively.

Therefore, equilibrium conditions are also established between the saturated vapor phase and the adsorbed phase. This can be expressed in terms of the equivalence of fugacity of each component in all the three phases, which is given below in equation 1.

$$f_i^{vap}(T, P^s, y_i) = f_i^{liq}(T, P^s, x_i) = f_i^{ads}(T, P^s, x'_i) \tag{1}$$

Here, f_i^{vap}, f_i^{liq} and f_i^{ads} are the fugacity of the component i in the vapor, liquid and adsorbed phase, respectively. The equilibrium conditions for the vapor-liquid equilibrium and adsorption equilibrium are the temperature T and the saturation pressure P^s, which is the mixture bubble point pressure at the temperature T.

At equilibrium, the surface excess of component 1 in the adsorbed phase , ${n_1}^e$, is given by equation 2 [28]

$$n_1^e = n'(x_1' - x_1) \tag{2}$$

Here, n' is the total number of moles adsorbed onto the adsorbent surface, x_1' and x_1 are the equilibrium mole fractions of component 1 in the adsorbed phase and the bulk liquid phase, respectively. The surface excess of each component can be determined experimentally by measuring the mole fraction of each component in the bulk liquid phase, before and after adsorption [28].

Based on the aforementioned equilibrium between the three phases, it has been shown previously [20] that the surface excess of components 1 can also be obtained from the experimental data of adsorption of the unsaturated vapor mixture of components 1 and 2, by the following relation given in equation 3.

$$n_1^e = \lim_{P \to P^s} n'(x_1' - x_1) \tag{3}$$

Thus, the adsorption of the binary liquid mixture can also be considered as the adsorption of the corresponding vapor mixture, in the limit of the pressure approaching the saturation pressure P^s of the liquid mixture at the given temperature . The methods used in this work to estimate the surface excess of binary liquid adsorption are described in the next sections.

2.2 Adsorbed solution theory (AST)

Following the discussion in the previous section, the problem of computing the equilibrium surface excess of component 1 of the binary liquid mixture as shown in Figure 1 can be reformulated as the problem of computing the equilibrium amounts adsorbed for each component from the corresponding binary vapor mixture. Therefore, the thermodynamic framework of the adsorbed solution theory can be applied in this context. As per the real adsorbed solution theory (RAST), [24, 29–31] the equilibrium between the vapor phase and the adsorbed phase can be described by a modified Raoult's law type expression given by equation 4.

$$P^s y_i = P_i^0(T,\pi) x_i' \gamma_i'(T,\pi,x_i') \tag{4}$$

Here, P_i^0 is the pure adsorbate vapor pressure at the system temperature T and spreading pressure π [29]. The activity coefficient γ_i' represents the non-ideality of the adsorbed phase. For an ideal adsorbed phase, the activity coefficient is unity. The meaning of all other variables has been described in the previous section. Thus, equation 4 can be used to calculate the amount adsorbed x_1' for the component 1, which is needed for the surface excess calculation in equation 2. The value of the total amount adsorbed, n' is also required in the surface excess calculation. This value can be calculated using an expression from the ideal adsorbed Solution Theory (IAST) [29], given in equation 5.

$$\frac{1}{n'} = \frac{x_1'}{n_1'(P_1^0)} + \frac{x_2'}{n_2'(P_2^0)} \tag{5}$$

Here, $n_i'(P_i^0)$ is the amount adsorbed for pure component i at the system temperature and pure adsorbate vapor pressure P_i^0. This expression has been derived by an expression for the change in the area due to mixing, Δa^m, at constant at T and π [29], given by equation

$$\begin{aligned} \Delta a^m(T,\pi,x_i',) &= a(T,\pi,x_i') - \sum_{i=1}^{2} x_i' a_i^0(T,\pi) \\ \Delta a^m(T,\pi,x_i') &= RT \sum_{i=1}^{2} x_i' \frac{\partial ln \gamma_i'}{\partial \pi} \end{aligned} \tag{6}$$

where, a represents the area of the adsorbent per mole of the total amount adsorbed, and a_i^o is the area of the adsorbent per mole of the pure adsorbate adsorbed at the system T and π. For an ideal adsorbed phase, the activity coefficient of each component is unity and therefore, the area change upon mixing at constant T and π is zero. Thus, equation 5 can be derived using equation 6 for an ideal adsorbed phase. For a real adsorbed phase, the area change upon mixing may or may not be zero. However, in the special case of adsorption from the liquid phase, or the corresponding adsorption from its saturated vapor phase, the surface coverage is

high (*see* § *3.2* for a detailed discussion). Therefore, at high loading which in the current case corresponds to the relative pressure of unity, the activity coefficient will be a weak function of the spreading pressure [32]. Thus, the change in the area due to mixing would be negligible and equation 5 could still be applied to a real adsorbed phase.

The utility of equations 4 and 5 depends on the computation of the other variables involved in both the equations. The vapor phase compositions y_i and saturation pressure P^s corresponding to the given liquid phase compositions x_i and temperature T were calculated using experimental vapor-liquid equilibrium data. These calculations were performed by regressing the parameters of the NRTL model [27] in Aspen Properties® V11 (*described in the* § *2.4*).

In this work, the generalized Langmuir isotherm model (gL) [26] (*see* § *2.3*) was used to calculate the equilibrium amount adsorbed as a function of pressure for each pure component constituting the binary mixture, using the available experimental data for pure vapor adsorption [6,18]. The spreading pressure of each pure component was subsequently computed as a function of vapor phase pressure using the Gibbs adsorption isotherm equation [29] given below.

$$\frac{d\pi_i}{dlnP} = \frac{n_i'' RT}{A^o} \tag{7}$$

Here, n_i'' is the equilibrium amount adsorbed for the pure component i at the pressure P, which is calculated with the gL model and A^o is the surface area of the adsorbent. At equilibrium and as per the framework of AST [29],

$$\pi_{mixture} = \pi_1 = \pi_2 \tag{8}$$

Thus, the spreading pressure of the mixture was computed to satisfy the relation of equation 8. The mixture spreading pressure was required to compute the values of P_i^0 and $n_i'(P_i^0)$.

The activity coefficient of each component in the adsorbed phase was calculated using the aNRTL model [25]. This thermodynamically consistent model has been successful in representing both ideal and non-ideal behavior of binary gas adsorption as functions of the

adsorbed phase mole fractions and temperature for different homogeneous and heterogeneous adsorbents, respectively [25,33]. Using the theory of local compositions [27,34], the expressions for the activity coefficient of each component were derived [25] and are given by equation 9.

$$ln\gamma_1' = \frac{x_2'^2\tau_{12}'[G_{12}' - 1]}{[x_1'G_{12}' + x_2']^2}, \quad ln\gamma_2' = \frac{x_1'^2\tau_{21}'[G_{21}' - 1]}{[x_2'G_{21}' + x_1']^2} \tag{9}$$

Where, $\tau_{12}' = -\tau_{21}'$ and $G_{12}' = exp(-\alpha\tau_{12}')$, τ_{12}' is the binary interaction parameter of the aNRTL model and α is the non-randomness factor, set to the value of 0.3, in conjunction with the NRTL model [27]. The reference state for the aNRTL model is the pure adsorbate at system temperature and spreading pressure of the mixture. This is equivalent to the component activity coefficient being unity at the component mole fraction of unity [25]. The binary interaction parameter was regressed using the experimental data for the surface excess. The maximum likelihood objective function [35] used for the regression is given in equation 10.

$$f = \sum_{r=1} \left(\frac{n^e_{1,calc,r} - n^e_{1,exp,r}}{\sigma_{exp}} \right)^2 \tag{10}$$

Here, $n^e_{1,calc}$ and $n^e_{1,exp}$ refer to the calculated and experimental surface excess amounts of component 1 while σ_{exp} is the standard deviation in the measurement of surface excess and is set to 0.05 mol/kg; r is the index for the experimental data points.

The detailed algorithm for the application of the Adsorbed Solution Theory to model the equilibrium adsorption for a binary liquid mixture is shown in Figure 2. The same algorithm was also used to predict the surface excess using IAST, by fixing the τ_{12}' parameter to 0.

2.3 Generalized Langmuir isotherm (gL)

The second method for the calculation of surface excess of binary liquid adsorption is the generalized Langmuir isotherm model (gL) [26] . This model is an extension and generalization of the thermodynamic Langmuir isotherm model (tL) for pure component isotherms [33,36,37]. The tL model incorporates the adsorbent heterogeneity by assigning phantom molecules ϕ to the vacant sites of the adsorbent and also expresses the adsorption-desorption equilibria in

terms of the activities of the adsorbed and the phantom molecules, as opposed to concentration of the same used in the classical Langmuir model [38].

The gL model extends this concept for multicomponent adsorption equilibria and further generalizes it by taking into account the variation of the saturation loadings of the pure adsorbates on the same adsorbent at the system temperature. This variation arises due to difference in size between a pure adsorbate molecule and the phantom molecule corresponding to the vacant site of the adsorbent. The gL model addresses this physical reality by considering a constant total surface area of the adsorbent, which can be expressed in terms of the saturation loading and molecular cross-sectional area of the adsorbate molecule. The gL model is applicable for both pure component and mixed-gas adsorption equilibria.

The surface area of adsorption for a given adsorbent is usually reported in the literature. The cross-sectional area of the adsorbate molecules on the adsorbent at the given temperature is also obtained from the literature. The phantom molecule is chosen to be the nitrogen molecule. Thus, the total area of the adsorbent is given as follows,

$$A^o = n_i''^0 A_i = n_\phi''^0 A_\phi \tag{11}$$

where, A^o is the area of the adsorbent, $n_i''^0$ and $n_\phi''^0$ are the saturation loadings of the component i and phantom molecule ϕ, respectively; A_i and A_ϕ are the corresponding molecular cross-sectional areas.

Thus, for pure component or mixed-gas adsorption consisting of m adsorbates, the area fractions of the adsorbed and phantom molecules can be computed by the following equations,

$$\theta_i'' = \frac{n_i'' A_i}{A^o} = \frac{n_i''}{n_i''^0} = \frac{K_i^o y_i P}{\frac{\gamma_i''}{\gamma_\phi'' q_i} + \sum_{j=1}^{m} \frac{\gamma_i'' q_j}{\gamma_j'' q_i} K_j^o y_j P} \tag{12}$$

$$\theta_\phi'' = \frac{n_\phi'' A_\phi}{A^o} = \frac{n_\phi''}{n_\phi''^0} = \frac{1}{1 + \sum_{j=1}^{m} \frac{\gamma_\phi'' q_j}{\gamma_j''} K_j^o y_j P} \tag{13}$$

Where, $q_i = A_i/A_\phi$, θ_i'' and θ_ϕ'' are the area fractions of the i^{th} adsorbate and the phantom molecule, respectively; n_i'' and n_ϕ'' are the corresponding amounts adsorbed. The activity coefficients of the adsorbed and phantom molecules are γ_i'' and γ_ϕ'', respectively. The equilibrium constant for the pure i^{th} component is K_i^o. The mole fraction of the i^{th} component in the bulk vapor phase is y_i and the total pressure in the vapor phase is given by P. In the case of binary liquid adsorption, P is replaced by P^s, the bubble point pressure of the liquid mixture at the temperature T. Thus, according to equations 12 and 13, mixed gas adsorption containing m components is treated as adsorption of $m+1$ components. In other words, pure component adsorption is treated as binary adsorption consisting of the pure adsorbate and the phantom molecule. Similarly, binary gas adsorption is treated as adsorption of the ternary system, containing two adsorbate molecules and one phantom molecule.

The activity coefficients used in equations 12 and 13 are computed by a modified aNRTL model, which takes into account the adsorbent heterogeneity and the size of the molecules [26]. The equation for the activity coefficient of the modified aNRTL is given in equation 14. For the case of binary vapor adsorption, $i, j, k = 1, 2, \phi$. Thus, there will be three activity coefficients for the binary vapor adsorption, γ_1'', γ_2'' and γ_ϕ''.

$$ln\gamma_i'' = q_i \frac{\sum_{j=1}^{m} x_j''^2 q_j^2 \tau_{ij}'' [G_{ij}'' - 1]}{(\sum_{k=1}^{m} x_k'' q_k G_{kj}'')^2} \tag{14}$$

Where, $\tau_{ij}'' = -\tau_{ji}''$, $\tau_{ii}'' = 0$, $G_{ij}'' = \exp(-\alpha\tau_{ij}'')$, γ_i'' is the activity coefficient in the adsorbed phase. The true mole fractions in the adsorbed phase are x_j'' and x_k'' and the binary interaction parameter is τ_{ij}''. For the case of binary gas adsorption, the calculations of the true mole fractions of the adsorbate molecules in the adsorbed phase, x_1'' and x_2'', include the contribution of the phantom molecule. Hence, in order to compare the calculated mole fractions with the experimental mole fractions, the apparent mole fractions, x_1' and x_2' are calculated as given below.

$$x_1' = \frac{x_1''}{x_1'' + x_2''}, \quad x_2' = \frac{x_2''}{x_1'' + x_2''} \tag{15}$$

Thus, in the case of binary liquid adsorption, the expression for the surface excess using gL model is given below and has the same mathematical form as equation 2.

$$n_1^e = n'(x_1' - x_1) \tag{16}$$

In equation 16, $n' = n_1'' + n_2''$. For the case of pure component adsorption, given the values of A^o and A_i in the literature, the gL model requires only two adjustable parameters, K_i^o and $\tau_{i\phi}''$. Hence, using the evaluated pure component isotherm parameters, the mixed gas adsorption using the gL model requires only one adjustable parameter, τ_{12}''. The regression of the τ_{12}'' parameter for the adsorption of saturated binary vapor mixture corresponding to the binary liquid mixture is performed by minimizing the objective function given in equation 10.

The computational load for the gL model is very low, in contrast to the RAST and IAST frameworks, where most of the computational time is spent on satisfying the spreading pressure constraint of equation 8. Furthermore, the gL model has been shown to significantly improve the correlations of IAST, RAST and extended Langmuir for mixed gas adsorption [26]. The detailed algorithm for the implementation of the gL model applied to the adsorption of the binary liquid mixture is shown in Figure 3. It is to be noted that the algorithm to evaluate the pure component parameters for pure component isotherm is the same as that provided in the gL model [26].

2.4 Vapor-liquid Equilibria (VLE)

The vapor phase composition corresponding to each binary liquid mixture was estimated using the NRTL activity coefficient model in Aspen Properties ® V11. The experimental data used in the regression of the binary interaction parameter of the NRTL model was retrieved from the Aspen Properties ® V11 database. The experimental data consisted of isothermal PXY data (293 - 360 K) and isobaric TXY data (0.39 - 1 bar). The details of the experimental data used in this work are provided in the Tables S1-S7 of the Supplementary Information. The regressed binary interaction parameters of the NRTL model were incorporated in the Flash calculations at 303 K to generate the vapor phase composition and saturation pressure corresponding to the given liquid phase composition for each binary system. Thus, this set of data was subsequently

used as an input to the code, which computed the surface excess of each binary system using the IAST, RAST and gL frameworks.

3. RESULTS AND DISCUSSION

3.1 Estimations of vapor phase composition and saturation pressure

The six binary liquid mixtures studied in this work are: *i*) benzene (1)−1,2-dichloroethane (2), *ii*) benzene (1)−cyclohexane (2), *iii*) cyclohexane (1)−1,2-dichloroehtane (2), *iv*) benzene (1)−n-heptane (2), *v*) cyclohexane (1)−n-heptane (2), *vi*) 1,2-dichloroethane (1)−n-heptane (2). The experimental data of the surface excess of the six binary liquid mixtures adsorbed on silica gel at 303 K was taken from the previous studies [6, 18].

The details of the regressed binary interaction parameters of the NRTL model are shown in Tables S8-S9. The comparison of the NRTL model correlations of the PXY data to the experimental data of the same at different temperatures for each binary system is shown in Figure S1. It can be seen from Figure S1 that the correlation of isothermal VLE data at different temperatures agrees well with the corresponding experimental data for all the systems. Moreover, the Root-Mean-Square-Error of the regression is very low for all the systems (See Table S8). Therefore, it can be concluded that the NRTL activity coefficient model is suitable for the calculation of the vapor phase composition and saturation pressure for each binary liquid mixture at 303 K.

3.2 Correlations of pure component isotherms

Table 1: **Pure component gL parameters for adsorption on silica gel at 303 K**. *P_i^s is the saturation pressure of the pure adsorbate, A^o is the surface area of adsorbent reported in the literature [18], $n_i''^0$ is regressed from the experimental isotherms and $A_i = A^o/n_i''^0$; The area of n-heptane has been adjusted by 20% from the original case [39] and the two gL parameters are regressed (n-heptane(adj.)).*

Adsorbates	P_i^s (bar)	A_i $(nm^2/molecule)$	A^o (m^2/g)	$n_i''^0$ (mol/kg)	$\tau_{i\phi}''$	K_i^o (bar^{-1})	RMSE (mol/kg)	ARD (%)	Ref. (Exp.)
1,2-dichloroethane	0.13	0.248	660	4.42±0.04	-1.73±0.07	111.97±3.21	0.17	8.00	[18]
benzene	0.16	0.251	660	4.35±0.02	-1.42±0.03	73.24±1.60	0.10	5.37	[6]
cyclohexane	0.16	0.296	660	3.7±0.02	0±0.06	26±0.26	0.13	9.25	[6]
n-heptane	0.075	0.430	660	2.55±0.05	-0.55±0.34	102.25±4.26	0.06	9.83	[6]
n-heptane (adj.)	0.075	0.350	660	3.13	-1.52±0.02	55.19±0.53	0.15	8.70	[6]

The pure component gL parameters of the four adsorbates (1,2-dichloroethane, benzene,

cyclohexane, n-heptane) adsorbed on silica gel at 303 K were regressed using experimental pure vapor isotherms [6, 18]. These parameters were required to compute the spreading pressure of each component as a function of the pressure *(see equation 7)*. The spreading pressure of the mixture required for the IAST and RAST frameworks was evaluated to satisfy the contraint of equation 8. These parameters were also needed in the input of the binary gL code as shown in Figure 3. The pure component isotherm parameters are tabulated in Table 1. The plot of pure component spreading pressure as a function of the pressure is given in Figure S2A.

The plot of the vacant site area fraction as a function of the relative pressure is given in Figure S2B. This has been calculated using the gL model [26] for the pure component adsorption. It can seen from Figure S2B that more than 80% area of the surface is covered by the pure adsorbate molecules at the relative pressure of unity. Since pure vapor adsorption at the relative pressure of unity is the limiting case of binary liquid adsorption, we can conclude that the surface coverage is high for the case of binary liquid adsorption, and the activity coefficients (γ_i'') are weakly dependent on the spreading pressure and approach a constant value [32], validating the use of equation 5 for RAST.

The surface area of silica gel, A^o, which was used for the measurements of the pure vapor isotherms of the four adsorbates and the subsequent surface excess of the corresponding binary liquid mixtures was reported to be 660 m^2/g in the literature [18]. The molecular cross-sectional area of each of the four adsorbates, A_i, was calculated using equation 10 by regressing the saturation loading $n_i''^0$ of each pure adsorbate on silica gel, using experimental pure vapor isotherm data [6, 18].

There were three methods reported in the literature [40] for the calculation of the molecular cross-sectional area of the adsorbate molecules. The first method involved using the two-dimensional (2D) Van der Waals constant, b', calculated using the critical properties of the component [41]. However, this method was based on the assumption of the applicability of the Van der Waals equation of state to the vapor phase and the adsorbed phase [41]. The second method used liquid density values of the components at 303 K and the assumption of spherical molecules, with hexagonal packing [40]. Hence, the first two methods were not very robust due to the simplifying assumptions involved in the calculation of A_i. The third method incorporated the use of the adsorption measurements from different sources to calculate the molecular cross-

sectional area of the four adsorbates [40]. However, this method lacked consistency as silica gel is an amorphous adsorbent and therefore, the structure of the porous network would vary with the synthesis process and the manufacturer. Thus, different sources/research groups reported drastically different A_i values for the same adsorbate-adsorbent system at any given temperature [40].

In this work, a comparison and analysis of the gL representation of the pure vapor isotherms was performed for all the three methods of computing the molecular cross-sectional area of the adsorbates. This is shown in Figure S3 and Table S10. It can be seen in Table S10 that the average relative deviation (ARD) (see equation 17) of the pure gL correlations at 303 K involving the calculation of A_i using the first two methods (Van der Waals constant and liquid density) was more than 10% for all the four adsorbates. Moreover, the pure gL correlations with A_i calculated using the third method (adsorption experiments) and reported in the literature [40] resulted in ARD$>$ 15% for all the four adsorbates. Thus, in this work, the regression of $n_i''^0$ and hence the calculation of the molecular cross-sectional area of the adsorbates, A_i, was deemed necessary. Thus, there were three pure gL parameters regressed in this work from the experimental pure vapor isotherms for each of the four adsorbates [6, 18].

It can be seen in Figure 4 that the representation of the pure component isotherms using the gL model is in line with the experimental data [6, 18] for all the systems, with the average relative deviation (ARD) $\leq$ 10% in all of the four cases (see Table 1). Moreover, the area of n-heptane has been adjusted by 20% from 0.43 $nm^2/molecule$ to 0.35 $nm^2/molecule$ to examine the effect of the cross-sectional molecular area value on the binary surface excess correlations, which is explained in the next subsection. The value of 20% is based on a recent systematic investigation by Cai et al. [39] who suggested the uncertainties associated with experimental data of pure and binary mixture loadings to be $\pm$20%. The corresponding pure gL parameters for n-heptane are tabulated in Table 1, with the ARD further reduced to 8.70% as opposed to 9.83% in the original case. The representation of this case is shown by the dashed line in Figure 4.

Table 2: **Binary interaction parameters of the IAST, RAST and gL frameworks for adsorption of binary liquid mixtures on silica gel at 303 K**. *Here the molecular cross-sectional area of n-heptane is 0.43 nm^2/molecule calculated using regressed $n_i''^0$ from the pure vapor isotherms.*

	IAST			RAST			gL		
System	τ'_{12}	**ARD (%)**	**RMSE**	τ'_{12}	**ARD (%)**	**RMSE**	τ''_{12}	**ARD (%)**	**RMSE**
benzene (1) – 1,2-dichloroethane (2)	0	61.90	0.05	0.40±0.13	57.45	0.05	0.26± 0.13	26.07	0.020
benzene (1) – cyclohexane (2)	0	14.42	0.12	-0.90±0.04	17.41	0.15	0±0.06	37.50	0.41
cyclohexane (1) – 1,2-dichloroethane (2)	0	29.17	0.07	1.38±0.26	27.25	0.03	-0.01±0.06	43.32	0.23
benzene (1) – n-heptane (2)	0	16.30	0.11	-1.20±0.09	16.10	0.16	-1.05±0.03	93.44	0.92
cyclohexane (1) – n-heptane (2)	0	–	0.007	-0.24±0.37	–	0.007	-0.58±0.07	–	0.03
1,2-dichloroethane (1) – n-heptane (2)	0	25.43	0.18	0±0.02	21.37	0.13	0±0.03	99.80	0.99

3.3 Correlations of Surface Excess - AST and gL Results

The binary interaction parameters of the IAST and RAST frameworks and the gL model for the adsorption of the six binary liquid mixtures on silica gel at 303 K are shown in Table 2. It also contains information on the average relative deviation (ARD) and the root-mean-square-error (RMSE) of the regression, both calculated for N experimental data points, which are defined as follows,

$$ARD = \frac{100}{N}\sum_{j=1}^{N}\left|\frac{n^e_{1,calc,j} - n^e_{1,exp,j}}{n^e_{1,exp,j}}\right| \tag{17}$$

$$RMSE = \sqrt{\frac{\sum_{j=1}(n^e_{1,calc,j} - n^e_{1,exp,j})^2}{N}} \tag{18}$$

The surface excess of the binary system of benzene (1)−1,2-dichloroethane (2) on silica gel at 303 K is shown in Figure 5. It can be seen from Figure 5 that 1,2-dichloroethane is the preferentially adsorbed component on silica gel at 303 K. Therefore, the surface excess of benzene is negative. This trend in the surface excess is captured by all the three frameworks,

IAST, RAST and gL, wherein the correlation of the gL model agrees well with the experimental data [18].

The correlations of the IAST and RAST frameworks are nearly same, with both of them overestimating the surface excess throughout the entire liquid phase composition of benzene. The average relative deviation of the correlations is 62% and 57%, respectively. The gL model has a lower ARD of 26% as opposed to the AST frameworks. Previously, Sircar and Myers [21] have derived an expression using Statistical Thermodynamics for the prediction of surface excess of binary liquid mixtures assuming an ideal adsorbed phase. The surface excess expression provided a quantitative fit to the experimental surface excess of benzene (1)− 1,2-dichloroethane (2) on silica gel at 303 K [21].

In this work, the binary interaction parameters of the RAST and gL model are 0.40 and 0.26 (see Table 2), which are indicative of small deviations from ideality. Moreover, the pure component isotherms and the spreading pressure plot shown in Figure 4 and Figure S2, respectively, indicate that 1,2-dichloroethane is slightly more adsorbed on silica gel at 303 K than benzene [18] for relative pressure values ranging from 0 to 1. Thus, the absolute value of the surface excess is small and this is also captured by all the three frameworks in this study. Thus, all the three frameworks successfully represented the surface excess of benzene (1)−1,2-dichloroethane (2) binary system on silica gel at 303 K and the gL model correlations agree with the previous modeling results and the experimental data for this system [18, 21].

The surface excess correlation of benzene (1)−cyclohexane (2) on silica gel at 303 K by all three frameworks is compared with the experimental data [6] of the same as shown in Figure 6.

In this case, the surface excess of benzene is positive, indicating that benzene is the preferred component over cyclohexane. The same can be inferred from the pure component adsorption isotherms of Figure 4 [6] and the spreading pressure plot of Figure S2. It has been shown previously that silica gel is a heterogeneous adsorbent for the adsorption of benzene (1)−cyclohexane (2) mixtures [23], indicating the non-ideality of the adsorbed phase [22]. This has been captured by RAST framework, with negative τ'_{12} parameters of -0.90 (See Table 2). However, the ARD of 17% for RAST is slightly higher than the ARD of 14% for IAST (See Table 2). This can be visually assessed from the plot of Figure 6. In contrast to both IAST and RAST which provide a good correlation of the experimental surface excess, the gL model

Table 3: **Binary interaction parameters of the gL framework for adsorption on silica gel at 303 K of three binary liquid mixtures, each with n-heptane as one component**. *Here the molecular cross-sectional area of n-heptane has been adjusted to 0.35 nm^2/molecule [39] (See Table 1 for pure gL parameters).*

	gL *(n-heptane(adj.))*		
System	τ''_{12}	**ARD (%)**	**RMSE**
benzene (1)−n-heptane (2)	-0.02±0.07	45.93	0.52
cyclohexane (1)−n-heptane (2)	-0.11±0.40	–	0.03
1,2-dichloroethane (1)−n-heptane (2)	0.004±0.02	61.09	0.57

captures the trend of the data, with a higher ARD of 37%.

The experimental data [18] and correlations of surface excess of cyclohexane (1)−1,2-dichloroethane (2) on silica gel at 303 K are shown in Figure 7.

The adsorption isotherms of Figure 4 indicate 1,2-dichloroethane to be strongly adsorbed on silica gel at 303 K than cyclohexane for all values of relative pressure. Hence the surface excess of cyclohexane is negative, as can be seen from the experimental data [18] and the correlations in Figure 7. This can be explained on the basis of the adsorption of the previous two binary systems on silica gel at 303 K: benzene (1)−1,2-dichloroethane (2) and benzene (1)−cyclohexane (2). Since, 1,2-dichloroethane is the preferred component over benzene (See Figure 5) and benzene is the preferred component over cyclohexane (see Figure 6), it makes sense that 1,2-dichloroethane would be the preferred component over cyclohexane (see Figure 7).

The correlations of surface excess from the frameworks of IAST and RAST agree with the experimental data [18], with RAST resulting in the best representation of the experimental data (see Table 2). The correlation of the gL model agrees qualitatively with the experimental surface excess data with ARD of 43%, similar to the benzene (1)−cyclohexane (2) binary adsorption.

The experimental surface excess data of benzene (1)−n-heptane (2) [6] along with the correlations of the three frameworks is shown in Figure 8. It can be seen that the trend of the positive surface excess of benzene in the experimental data is in line with the pure component isotherms of Figure 4 and spreading pressure plot of Figure S2. Moreover, both IAST and RAST correlations agree well with the experimental surface excess data.

The gL correlation, with n-heptane molecular area calculated using regressed $n_i''^0$ suggests azeotropic behavior at $x_1 = 0.58$. This is against the experimental surface excess data, where the silica gel preferentially adsorbs benzene for the entire range of bulk liquid compositions [6]. This was resolved by adjusting the area of n-heptane from 0.43 $nm^2/molecule$ to 0.35 $nm^2/molecule$, keeping the area of the adsorbent fixed at 660 m^2/g. Thus, with the new pure gL parameters of n-heptane (see Table 1), the gL model correlated the experimental surface excess data qualitatively with ARD reduced from 93% in the previous case to 45% (see Table 3). This also emphasizes the importance of the availability of accurate experimental data of the pure component isotherms required for the regression of pure gL parameters. Moreover, this result also signifies that, with the ±20% uncertainties associated with experimental data of pure and binary mixture [39], the pure gL parameters should be regressed by reconciling the pure and binary adsorption data simultaneously. It should be noted that the adjusted molecular cross-sectional area of n-heptane does not significantly change the results of the IAST and RAST frameworks for the adsorption of binary liquid mixture of benzene (1)−n-heptane (2) on silica gel at 303 K.

The surface excess of the cyclohexane (1)−n-heptane (2) mixture on silica gel at 303 K is shown in Figure 9. It can be seen that the experimental surface excess is 0 in this case [6]. This has been rationalized in a previous study [18] by the cross-over of the pure component isotherms of cyclohexane and n-heptane. Moreover, the spreading pressure plot of Figure S2 indicates the equality of the spreading pressure of the two pure components at a relative pressure of 1. This may result in the silica gel having no particular preference for either of the two components. This is also represented by the IAST and the RAST frameworks, in line with the previous work [21].

The gL model calculated a slight negative surface excess for cyclohexane. However, the gL correlations with the adjusted area of n-heptane resulted in negligible surface excess, thus representing the experimental data quite well (See Table 3). Thus, it once again highlights the significance of having accurate molecular area values of the adsorbates, by accounting both the pure and binary adsorption data. Similar to the previous case, the results of the IAST and RAST frameworks for the adsorption of binary liquid mixture of cyclohexane (1)−n-heptane (2) on silica gel at 303 K did not change significantly upon adjusting the molecular cross-sectional

area of n-heptane.

The experimental surface excess of 1,2-dichloroethane (1)−n-heptane (2) on silica gel at 303 K [18] with the correlated results are shown in Figure 10. The surface excess is positive for 1,2-dichloroethane for the entire range of liquid composition. The RAST framework has the least ARD of 21% in comparison to the experimental surface excess data, followed by IAST with ARD of 25%. Both the frameworks agree well with the experimental data.

The gL model suggests an azeotrope in the surface excess from $x_1 = 0.78$. However, the gL model correlation with the adjusted n-heptane molecular area of 0.35 $nm^2/molecule$ depicts a qualitative agreement with the experimental surface excess for a major part of the liquid mixture composition. It shows a small preference for n-heptane from $x_1 = 0.94$ onwards. The ARD was significantly reduced to 61% (See Table 3) after adjusting the n-heptane molecular area by 20%. Here, the results of the IAST and RAST frameworks were not affected significantly with the adjusted molecular area of n-heptane, in line with the previous two cases.

Interestingly, the binary interaction parameters of both RAST and gL correlations (original and adjusted n-heptane area) are 0 (See Tables 2 and 3) and thus, it can be concluded that the adsorbed phase of the binary liquid mixture of 1,2-dichloroethane (1)−n-heptane (2) on silica gel at 303 K is an ideal phase.

4. CONCLUSIONS

This work presents a comprehensive thermodynamic modeling approach for the adsorption of six binary liquid mixtures on silica gel at 303 K. The six liquid mixtures studied in this work are : *i*) benzene (1)−1,2-dichloroethane (2), *ii*) benzene (1)−cyclohexane (2), *iii*) cyclohexane (1)−1,2-dichloroehtane (2), *iv*) benzene (1)−n-heptane (2), *v*) cyclohexane (1)−n-heptane (2), *vi*) 1,2-dichloroethane (1)−n-heptane (2).

We have considered the adsorption from a binary liquid mixture to be equivalent to the adsorption from the corresponding saturated binary vapor phase. Therefore, using the available pure vapor isotherms of the components of the binary liquid mixtures, we have utilized the frameworks of the adsorbed solution theory [29] and the generalized Langmuir isotherm model (gL) [26] to compute adsorption from the saturated binary vapor phase. In the former approach, we have correlated the surface excess using both an ideal adsorbed phase (IAST) [29] and a real

adsorbed phase (RAST) [24,30,31] coupled with activity coefficients computed by the aNRTL model [25]. The composition of the binary vapor phase was estimated using the NRTL activity coefficient model [27] in Aspen Properties ® V11.

The correlations of the IAST and the RAST frameworks show a good agreement with the experimental surface excess data [6,18]. It can be inferred from the values of the aNRTL binary interaction parameters of each system, that the adsorbed phase for all six binary liquid mixtures adsorbed on silica gel is nearly ideal, with small deviations from Raoult's law behavior.

The gL model provides qualitative correlations for all six binary systems while requiring no computationally expensive spreading pressure calculations. Moreover, it was found in this study that the gL correlations of binary systems involving n-heptane as one component significantly improved after adjusting the molecular area value of n-heptane. This shows that the pure gL parameters should be regressed by reconciling the pure and binary isotherm data simultaneously. It also highlights the importance of the availability of accurate experimental data of pure component isotherms. The binary interaction parameters regressed from the gL model are close to zero, indicating an ideal adsorbed phase for all six binary systems which is in line with the IAST and RAST frameworks.

Our thermodynamic framework presented in this work for liquid adsorption does not make any assumptions regarding the ideality or structure of the adsorbed phase and the heterogeneity of the adsorbent, and it should be very useful in process simulations of separation processes based on liquid adsorption. Our future work will extend and apply this framework to the adsorption of other liquid mixtures on adsorbents for industrially relevant separations.

5. ACKNOWLEDGMENTS

Funding support is provided by the U. S. Department of Energy under the grant DE-EE0007888. The authors gratefully acknowledge the financial support of the Jack Maddox Distinguished Engineering Chair Professorship in Sustainable Energy sponsored by the J.F Maddox Foundation.

legal liability or responsibility for the accuracy, completeness, or usefulness of any information, apparatus, product, or process disclosed, or represents that its use would not infringe privately owned rights. Reference herein to any specific commercial product, process, or service by trade name, trademark, manufacturer, or otherwise does not necessarily constitute or imply its endorsement, recommendation, or favoring by the United States Government or any agency thereof. The views and opinions of authors expressed herein do not necessarily state or reflect those of the United States Government or any agency thereof.

AUTHOR CONTRIBUTIONS

Rajasi Shukre: Conceptualization, data curation, formal analysis, methodology, software, validation, visualization, and writing - original draft.

Shikha Bhaiya: Data curation, formal analysis, methodology, and validation.

Usman Hamid: Methodology, formal analysis, and software.

Hla Tun: Methodology and software.

Chau-Chyun Chen: Conceptualization, funding acquisition, investigation, methodology, project administration, resources, software, validation, , and writing - reviewing and editing.

REFERENCES

[1] Oak Ridge National Laboratory. Materials for separation technologies: Energy and emission reduction opportunities, 2005.

[2] JM Prausnitz, RN Lichtenthaler, and EG De Azevedo. *Molecular thermodynamics of fluid-phase equilibria*. Pearson Education, 1998.

[3] C Triantafyllou and R Smith. The design and optimization of dividing wall distillation columns. In *Energy Efficiency in Process Technology*, pages 351–360. Springer, 1993.

[4] MB Rao and S Sircar. Concentration swing adsorption: Novel processes for bulk liquid separations. In *Precision Process Technology*, pages 345–352. Springer, 1993.

[5] J Rouquerol, F Rouquerol, P Llewellyn, G Maurin, and KSW Sing. *Adsorption by powders and porous solids: principles, methodology and applications*. Academic press, 2013.

[6] DP Valenzuela and AL Myers. *Adsorption equilibrium data handbook*. Prentice Hall, 1989.

[7] DH Everett. Thermodynamics of adsorption from solution. part 1.—perfect systems. *Transactions of the Faraday Society*, 60:1803–1813, 1964.

[8] DH Everett. Thermodynamics of adsorption from solution. part 2.—imperfect systems. *Transactions of the Faraday Society*, 61:2478–2495, 1965.

[9] SG Ash, R Bown, and DH Everett. Thermodynamics of adsorption from solution. adsorption by graphon from binary mixtures of benzene, cyclohexane and n-heptane. *Journal of the Chemical Society, Faraday Transactions 1: Physical Chemistry in Condensed Phases*, 71:123–133, 1975.

[10] CE Brown, DH Everett, AV Powell, and PE Thorne. Adsorption and structuring phenomena at the solid/liquid interface. *Faraday Discussions of the Chemical Society*, 59:97–108, 1975.

[11] CE Brown, DH Everett, and CJ Morgan. Thermodynamics of adsorption from solution. the systems (benzene+ ethanol)/graphon and (n-heptane+ ethanol)/graphon. *Journal of the Chemical Society, Faraday Transactions 1: Physical Chemistry in Condensed Phases*, 71:883–892, 1975.

[12] G Schay and L Gy Nagy. Critical discussion of the use of adsorption measurements from the liquid phase for surface area estimation. *Journal of Colloid and Interface Science*, 38(2):302–311, 1972.

[13] I Dehany and LG Nagy. Some correlations of the equilibrium thermodynamics of the adsorption of liquid mixtures at solid-liquid interfaces. *Period. Polytech*, 19:485, 1978.

[14] DH Everett. Thermodynamics of adsorption from non-aqueous solutions. In *Progress in Colloid & Polymer Science*, pages 103–117. Springer, 1978.

[15] DH Everett and RT Podoll. Adsorption of near-ideal binary liquid mixtures by graphon. *Journal of Colloid and Interface Science*, 82(1):14–24, 1981.

[16] DH Everett. Thermodynamics of interfacial phenomena. *Pure and Applied Chemistry*, 53(11):2181–2198, 1981.

[17] S Sircar, J Novosad, and AL Myers. Adsorption from liquid mixtures on solids: Thermodynamics of excess properties and their temperature coefficients. *Industrial & Engineering Chemistry Fundamentals*, 11(2):249–254, 1972.

[18] AL Myers and S Sircar. Thermodynamic consistency test for adsorption of liquids and vapors on solids. *The Journal of Physical Chemistry*, 76(23):3412–3415, 1972.

[19] S Sircar and AL Myers. A thermodynamic consistency test for adsorption from binary liquid mixtures on solids. *AIChE Journal*, 17(1):186–190, 1971.

[20] AL Myers and S Sircar. Analogy between adsorption from liquids and adsorption from vapors. *The Journal of Physical Chemistry*, 76(23):3415–3419, 1972.

[21] S Sircar and AL Myers. Statistical thermodynamics of adsorption from liquid mixtures on solids. i. ideal adsorbed phase. *The Journal of Physical Chemistry*, 74(14):2828–2835, 1970.

[22] S Sircar and AL Myers. Prediction of adsorption at liquid-solid interface from adsorption isotherms of pure unsaturated vapors. *AIChE Journal*, 19(1):159–166, 1973.

[23] S Sircar. Thermodynamics of adsorption from binary liquid mixtures on heterogeneous adsorbents. *Journal of the Chemical Society, Faraday Transactions 1: Physical Chemistry in Condensed Phases*, 82(3):831–841, 1986.

[24] E Costa, JL Sotelo, G Calleja, and C Marron. Adsorption of binary and ternary hydrocarbon gas mixtures on activated carbon: experimental determination and theoretical prediction of the ternary equilibrium data. *AIChE Journal*, 27(1):5–12, 1981.

[25] H Kaur, H Tun, Ml Sees, and CC Chen. Local composition activity coefficient model for mixed-gas adsorption equilibria. *Adsorption*, 25(5):951–964, 2019.

[26] U Hamid, P Vyawahare, H Tun, and CC Chen. Generalization of thermodynamic langmuir isotherm for mixed-gas adsorption equilibria. *AIChE Journal*, page e17663.

[27] H Renon and JM Prausnitz. Local compositions in thermodynamic excess functions for liquid mixtures. *AIChE journal*, 14(1):135–144, 1968.

[28] JJ Kipling. *Adsorption from Solutions of Non-electrolytes*. Academic Press, 2017.

[29] AL Myers and JM Prausnitz. Thermodynamics of mixed-gas adsorption. *AIChE journal*, 11(1):121–127, 1965.

[30] AL Myers. Activity coefficients of mixtures adsorbed on heterogeneous surfaces. *AIChE journal*, 29(4):691–693, 1983.

[31] O Talu and I Zwiebel. Multicomponent adsorption equilibria of nonideal mixtures. *AIChE journal*, 32(8):1263–1276, 1986.

[32] FR Siperstein and AL Myers. Mixed-gas adsorption. *AIChE journal*, 47(5):1141–1159, 2001.

[33] H Tun and CC Chen. Prediction of mixed-gas adsorption equilibria from pure component adsorption isotherms. *AIChE Journal*, 66(7):e16243, 2020.

[34] GM Wilson. Vapor-liquid equilibrium. xi. a new expression for the excess free energy of mixing. *Journal of the American Chemical Society*, 86(2):127–130, 1964.

[35] HI Britt and RH Luecke. The estimation of parameters in nonlinear, implicit models. *Technometrics*, 15(2):233–247, 1973.

[36] CK Chang, H Tun, and CC Chen. An activity-based formulation for langmuir adsorption isotherm. *Adsorption*, 26(3):375–386, 2020.

[37] H Tun and CC Chen. Isosteric heat of adsorption from thermodynamic langmuir isotherm. *Adsorption*, 27(6):979–989, 2021.

[38] I Langmuir. The adsorption of gases on plane surfaces of glass, mica and platinum. *Journal of the American Chemical society*, 40(9):1361–1403, 1918.

[39] X Cai, F Gharagheizi, LW Bingel, D Shade, KS Walton, and DS Sholl. A collection of more than 900 gas mixture adsorption experiments in porous materials from literature meta-analysis. *Industrial & Engineering Chemistry Research*, 60(1):639–651, 2020.

[40] AL McClellan and HF Harnsberger. Cross-sectional areas of molecules adsorbed on solid surfaces. *Journal of Colloid and Interface Science*, 23(4):577–599, 1967.

[41] TL Hill. Statistical mechanics of multimolecular adsorption. iv. the statistical analog of the bet constant a 1 b 2/b 1 a 2. hindered rotation of a symmetrical diatomic molecule near a surface. *The Journal of Chemical Physics*, 16(3):181–189, 1948.

List of Figures

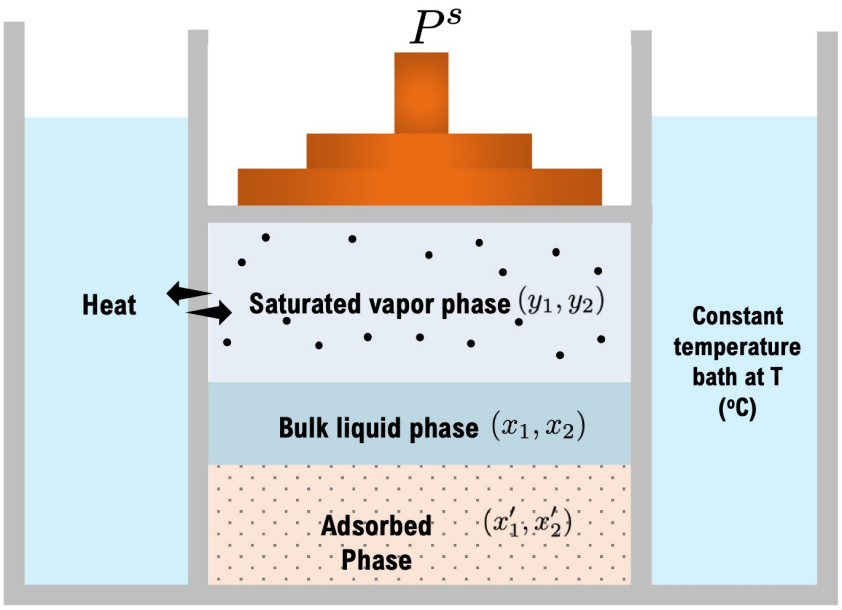

Figure 1: **Equilibrium Thermodynamic system for binary liquid mixture adsorption**

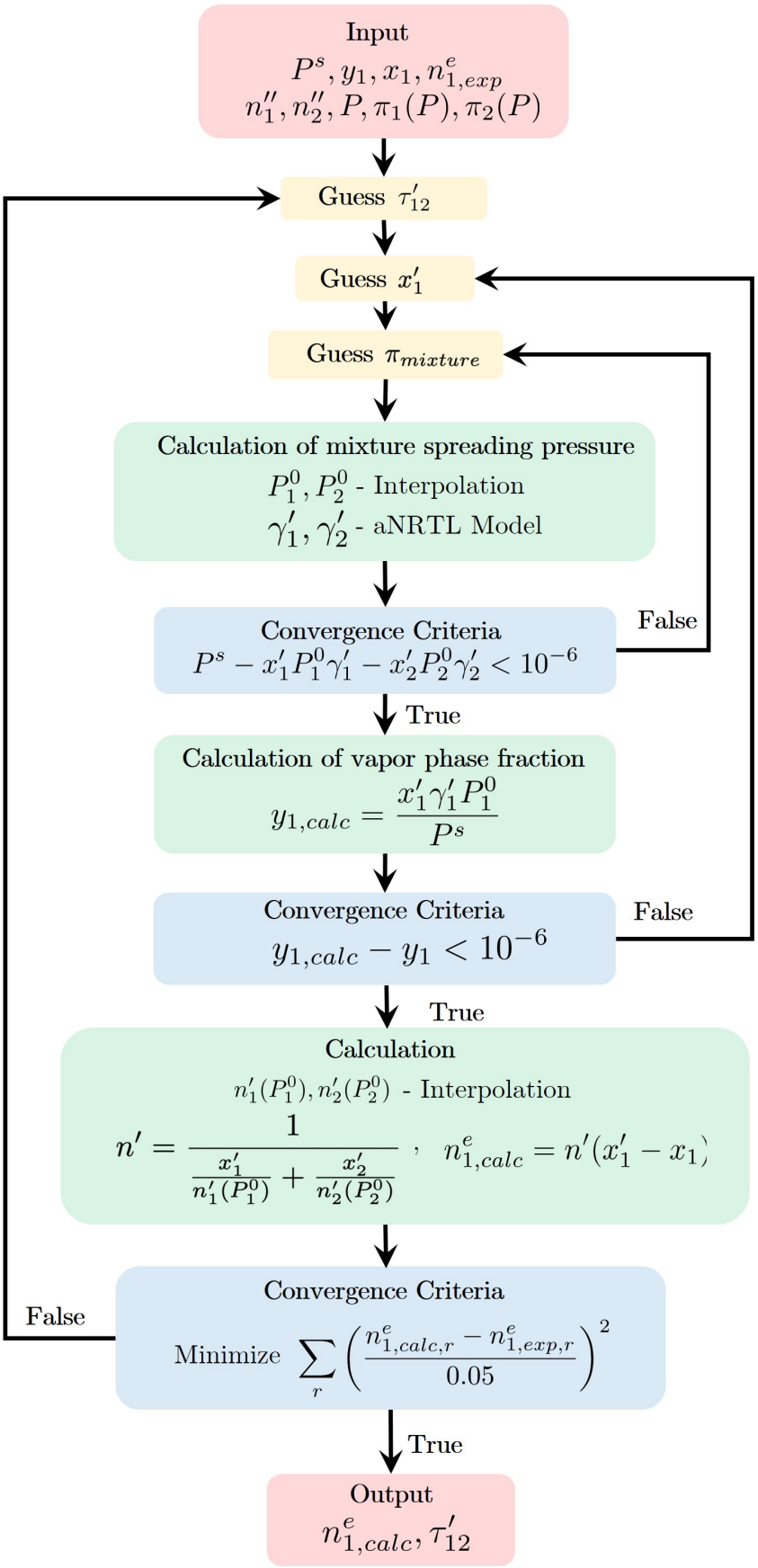

Figure 2: **Algorithm for prediction of adsorption from binary liquid mixtures using the AST framework**; *Here, r stands for the number of experimental data points, n''_1 and n''_2 are the amounts adsorbed for pure vapor components 1 and 2 for a given range of pressure (P) calculated using gL model.*

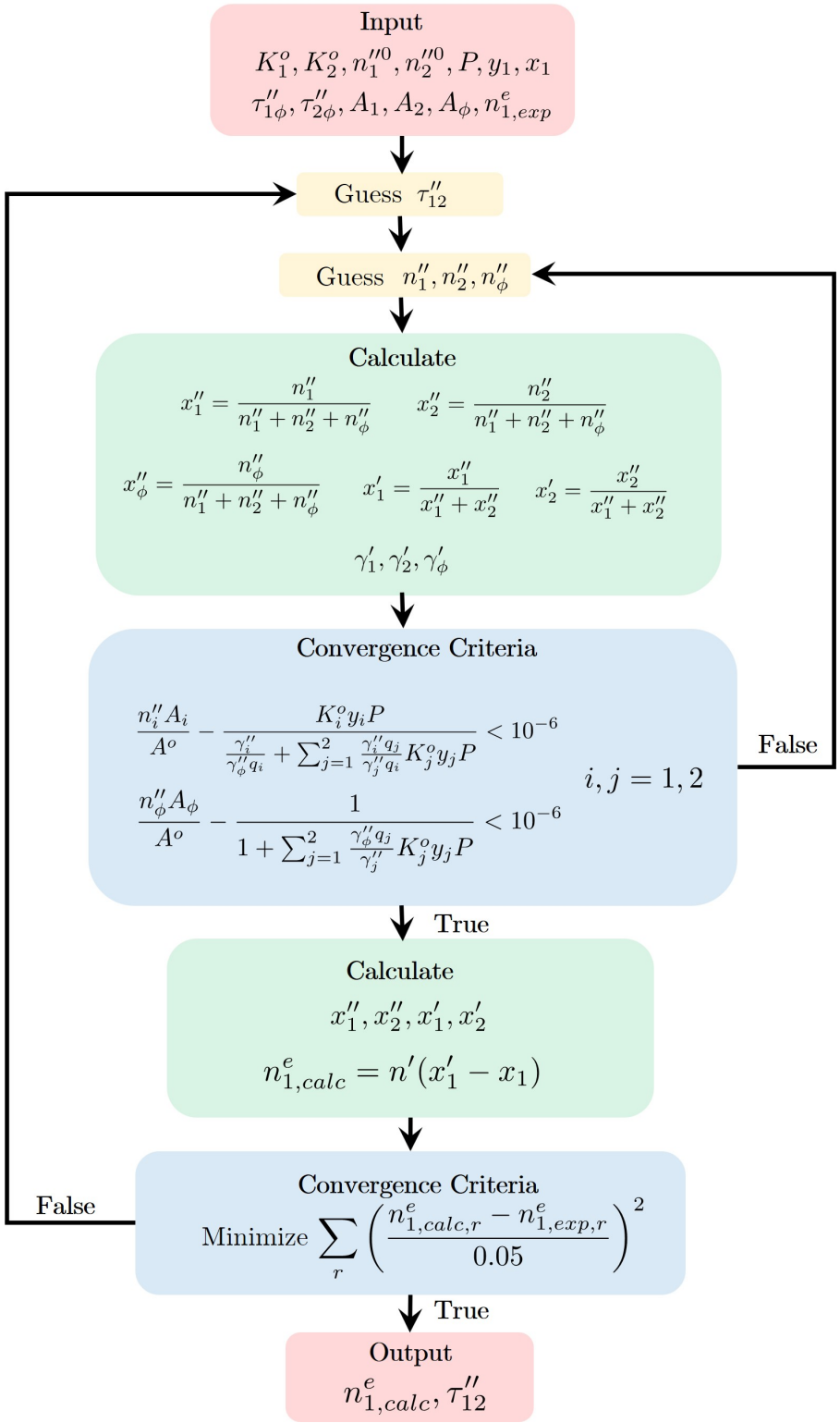

Figure 3: **Algorithm for prediction of adsorption from binary liquid mixtures using the gL Model**; *Here, r stands for the number of data points.*

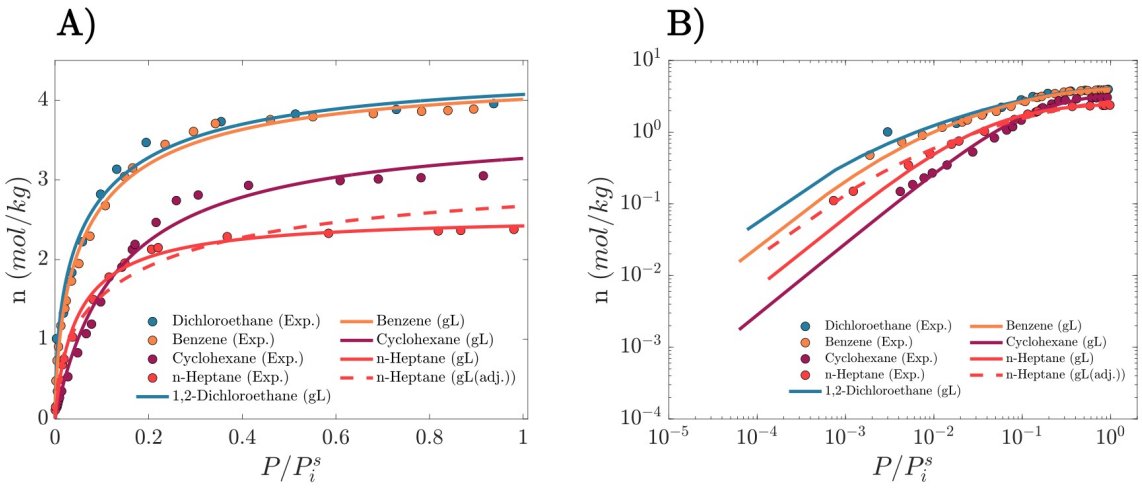

Figure 4: **gL Model correlations of pure component isotherms on silica gel at 303 K A) Linear scale B) Logarithmic scale**. *References for the experimental data are given in Table 1; P_i^s is the saturation pressure of pure adsorbate tabulated in Table 1,adj. refers to the adjusted area of n-heptane, with gL parameters given in Table 1.*

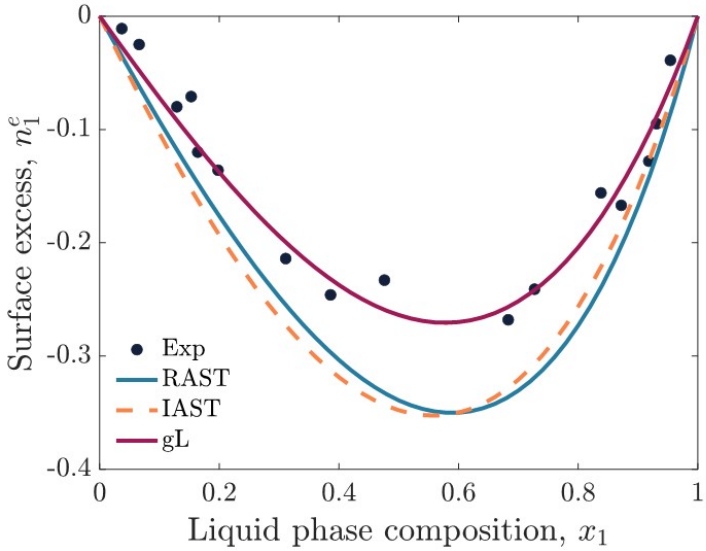

Figure 5: **Surface excess of benzene (1)−1,2-dichloroethane (2) mixture on silica gel at 303 K**; *Experimental data is from [18].*

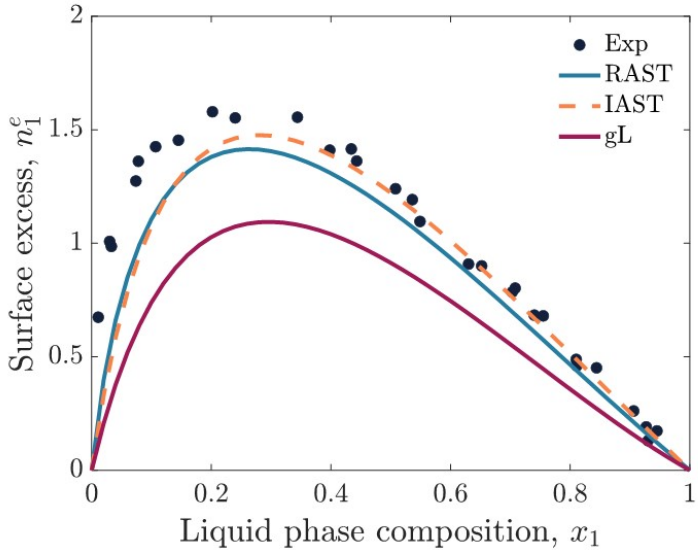

Figure 6: **Surface excess of benzene (1)−cyclohexane (2) mixture on silica gel at 303 K.**; *Experimental data is from [6].*

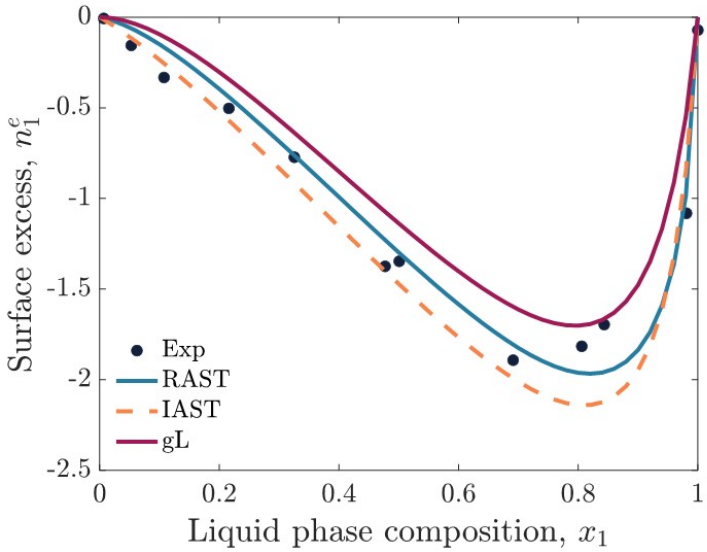

Figure 7: **Surface excess of cyclohexane (1)−1,2-dichloroethane (2) mixture on silica gel at 303 K.**; *Experimental data is from [18].*

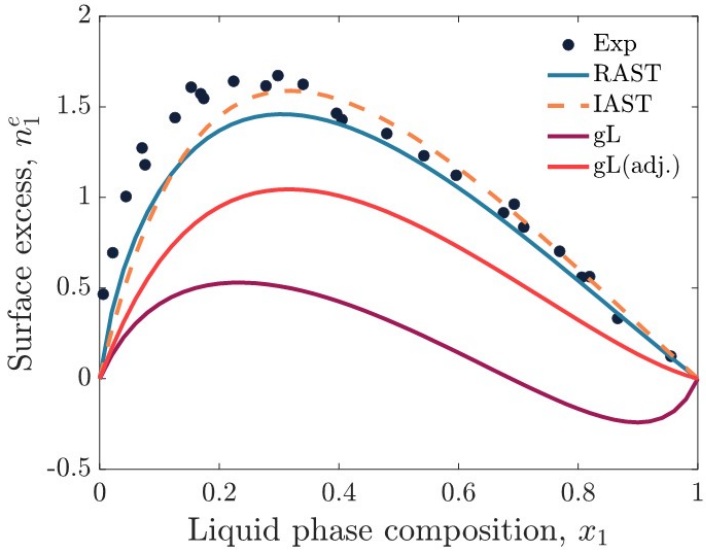

Figure 8: **Surface excess of benzene (1)−n-heptane (2) mixture on silica gel at 303 K.**; *Experimental data is from [6].*

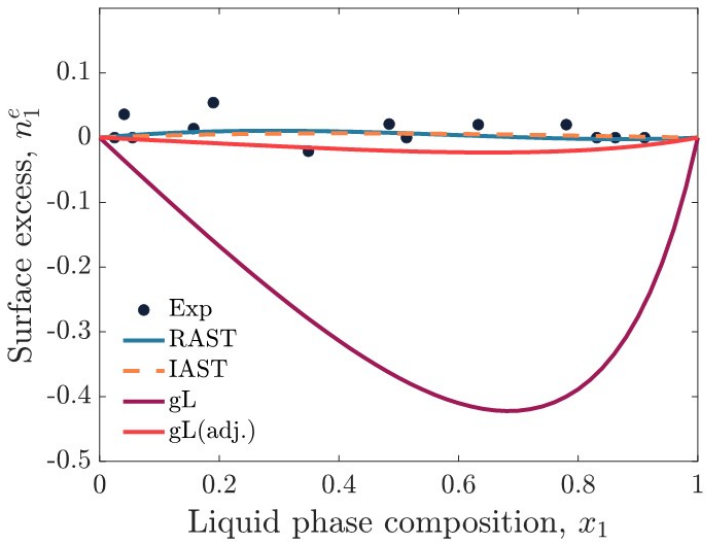

Figure 9: **Surface excess of cyclohexane (1)−n-heptane (2) mixture on silica gel at 303 K.**; *Experimental data is from [6].*

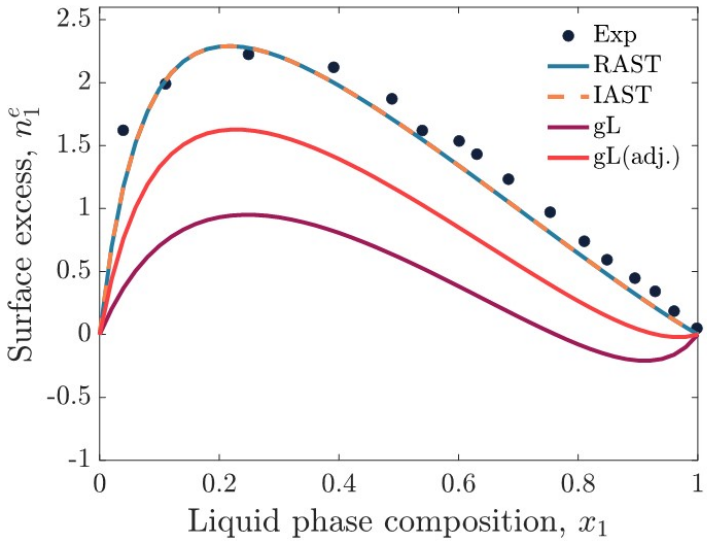

Figure 10: **Surface excess of 1,2-dichloroethane (1)−n-heptane (2) mixture on silica gel at 303 K**; *Experimental data is from [18].*